RAA 2018 Vol. **18** No. **11**, 131(10pp) doi: 10.1088/1674–4527/18/11/131

http://www.raa-journal.org *http://iopscience.iop.org/raa*

***R**esearch in*
***A**stronomy and*
***A**strophysics*

A new parametrization of dark energy equation of state leading to double exponential potential

Sudipta Das[1], Abdulla Al Mamon[2] and Manisha Banerjee[1]

[1] Department of Physics, Visva-Bharati, Santiniketan-731235, India; *sudipta.das@visva-bharati.ac.in*
[2] Department of Mathematics, Jadavpur University, Kolkata-700032, West Bengal, India

Received 2018 April 9; accepted 2018 May 15

Abstract We show that a phenomenological form of energy density for the scalar field can provide the required transition from decelerated ($q > 0$) to accelerated expansion ($q < 0$) phase of the universe. We have used the latest type Ia supernova (SNIa) and Hubble parameter datasets to constrain the model parameters. The best fit values obtained from those datasets are then applied to reconstruct $\omega_\phi(z)$, the equation of state parameter for the scalar field. The results show that the reconstructed forms of $q(z)$ and $\omega_\phi(z)$ do not differ much from the standard ΛCDM value at the current epoch. Finally, the functional form of the relevant potential $V(\phi)$ is derived by a parametric reconstruction. The corresponding $V(\phi)$ comes out to be a double exponential potential, which has a number of cosmological implications. Additionally, we have also studied the effect of this particular scalar field dark energy sector on the evolution of matter overdensities.

Key words: cosmic acceleration — quintessence field — dark energy density — perturbation

1 INTRODUCTION

Recent cosmological observations (Riess et al. 1998, 2004; Perlmutter et al. 1999; Eisenstein et al. 2005; Spergel et al. 2007) strongly suggest that the universe is currently going through an accelerated phase of expansion. These observations also suggest that the observed accelerated phase is indeed a very recent phenomenon and that the universe must have had a decelerated phase of expansion in the past in order to facilitate structure formation. The driving force responsible for generating this observed accelerated expansion is popularly named dark energy (DE), which has large negative pressure. For review on DE models, one can refer to the relevant review works (Sahni & Starobinsky 2000; Copeland et al. 2006; Martin 2008). Among the most popular DE models, the Λ cold dark matter (ΛCDM) model enjoys more worthy attention in the literature, and is found to be in good agreement with the observational data. But, it has two associated theoretical problems, namely, *fine tuning problem* and *cosmological coincidence problem* (Weinberg 1989; Steinhardt et al. 1999). Alternatively, quintessence models do not suffer from the above mentioned problems due to their dynamical nature and are widely used as candidates for DE. The quintessence (or canonical) field, is capable of driving the acceleration with some suitably chosen potentials, but none of these models have firm theoretical motivation (for a comprehensive review, see Sahni & Starobinsky 2000). Numerous DE models have been explored and studied over the last two decades in order to explain this observed late time accelerated behavior of the universe (for details, one can look into Sahni 2004). However, none of these models can be considered as superior to others, so the search is still on for a suitable model for DE consistent with the current observations. Although it is mostly believed that DE components do not cluster, recently studies have been conducted to investigate the effects of perturbations on DE components (Weller & Lewis 2003; Bartolo et al. 2004; Unnikrishnan 2008; Unnikrishnan et al. 2008; Jassal 2010), so this

branch of cosmology requires huge attention to probe whether such clustering can provide us with new information regarding the true nature of the DE component.

Keeping in mind the above facts, we have proposed a simple scalar field model of DE in the framework of a spatially flat ($k = 0$) Friedmann-Robertson-Walker (FRW) universe, where we have considered a functional dependence for the energy density of the scalar field, $\rho_\phi(a)$. The aim of this paper is to investigate the evolution history of the universe in this scenario. With this input, expressions for the Hubble parameter $H(z)$, deceleration parameter $q(z)$, equation of state (EoS) parameter $\omega_\phi(z)$ and density parameter $\Omega_\phi(z)$ are investigated. Next, we have obtained constraints on various parameters of the model using type Ia supernova (SNIa), Hubble and joint analysis of SNIa+Hubble datasets. The best-fit values obtained are then used to constrain the evolution behaviors of $q(z)$ and $\omega_\phi(z)$. We have found that for this specific ansatz, the deceleration parameter q smoothly transits from the positive to negative value regime in the recent past (around $z < 1$) such that structure formation can take place unhindered. These results are compatible with results that are expected both theoretically (Padmanabhan & Choudhury 2003; Choudhury & Padmanabhan 2005) and observationally (Riess et al. 2001, 2004; Turner & Riess 2002; Cunha 2009; Mamon & Das 2016). We also discuss the future evolution dynamics of the universe. Using the combination of the SNIa and Hubble datasets, we have also tried to obtain the functional dependence of potential $V(\phi)$ for this model. Finally, we also examine the effect of this particular DE sector on the growth of matter perturbations by comparing it with well studied cosmological models such as the ΛCDM model and Chevallier-Polarski-Linder (CPL) model or with a model where there is no DE sector.

The organization of the paper is as follows. In Section 2, we present basic equations related to the scalar field DE model for a spatially flat FRW model of the universe. We then obtain analytical solutions for the field equations using a specific choice of ρ_ϕ. In Section 3, we describe the observational datasets and their analysis method used in this paper. We then derive constraints on various cosmological parameters. The results are presented in Section 4. In Section 5, we study the effect of this particular DE sector on the evolution of matter overdensities at perturbative level. Finally, some conclusions are provided in Section 6.

2 THEORETICAL MODEL

The Einstein field equations for an FRW space-time (with a flat spatial term) are given by

$$3\frac{\dot{a}^2}{a^2} = \rho_m + \frac{1}{2}\dot{\phi}^2 + V(\phi) = \rho_m + \rho_\phi \,, \tag{1}$$

$$2\frac{\ddot{a}}{a} + \frac{\dot{a}^2}{a^2} = -\frac{1}{2}\dot{\phi}^2 + V(\phi) = -p_\phi \,, \tag{2}$$

written in natural units such that $8\pi G = c = 1$.
It is clear from Equations (1) and (2) that the energy density ρ_ϕ and pressure p_ϕ for the scalar field component are

$$\rho_\phi = \frac{1}{2}\dot{\phi}^2 + V(\phi) \ , \tag{3}$$

$$p_\phi = \frac{1}{2}\dot{\phi}^2 - V(\phi) \ . \tag{4}$$

Also, the conservation equations for the scalar field and matter field are

$$\dot{\rho}_\phi + 3H(\rho_\phi + p_\phi) = 0 \ , \tag{5}$$

$$\dot{\rho}_m + 3H\rho_m = 0 \ . \tag{6}$$

Equation (6) on integration yields

$$\rho_m = \rho_{m0} a^{-3} \ , \tag{7}$$

where ρ_{m0} denotes the current value of energy density corresponding to the matter field.

Also, from Equation (5), one can obtain the EoS parameter as

$$\omega_\phi = \frac{p_\phi}{\rho_\phi} = -1 - \frac{a}{3\rho_\phi}\frac{d\rho_\phi}{da} \ . \tag{8}$$

Only three equations among (1), (2), (5) and (6) are independent. The fourth one can be derived from the other three in view of the Bianchi identities. So, we have to solve for four unknown parameters, namely H, ρ_m, ϕ and $V(\phi)$, from three independent equations. Hence, an exact solution is not possible without an additional input. With this freedom, we make an ansatz for the functional form of ρ_ϕ as,

$$\frac{1}{\rho_\phi}\frac{d\rho_\phi}{da} = -\frac{\lambda a}{(k+a)^2} \ , \tag{9}$$

where k, λ are positive constants. This immediately yields,

$$\rho_\phi = \frac{A}{(k+a)^\lambda}\exp\left[-\frac{k\lambda}{(k+a)}\right] \ , \tag{10}$$

where $A = \rho_{\phi 0}(1+k)^\lambda \exp\left[\frac{k\lambda}{(1+k)}\right]$ and $\rho_{\phi 0}$ represents the current value of scalar field energy density. Of

course, the choice made in Equation (9) is quite arbitrary. However, for $k = 0$, Equation (10) will provide a simple power law evolution of ρ_ϕ ($\sim a^{-\lambda}$), which has been considered in many cosmological analyses (Copeland et al. 2006).

From Equations (8) and (9), one can immediately obtain the EoS parameter ω_ϕ as a function of redshift z ($z = \frac{1}{a} - 1$) as

$$\omega_\phi(z) = -1 + \frac{\lambda}{3[1 + k(1+z)]^2} \ . \tag{11}$$

In fact, one can reframe this particular phenomenological model or the phenomenological choice made in (9) in a different way as well. One can as well make a choice for the EoS parameter $\omega_\phi(z)$ as

$$\omega_\phi(z) = \omega_0 + \frac{\omega_1}{(\omega_2 + \omega_3 z)^2} \ , \tag{12}$$

and for proper choices of ω_0, ω_1, ω_2 and ω_3 one can get back Equation (11).

Equation (12) provides a new form of parametrization for the DE EoS parameter. It deserves mention that for proper choices of λ and k in Equation (11), or equivalently for $\omega_2 = \omega_3 = 1$, Equation (12) takes the form

$$\omega_\phi(a) = \omega_0 + \omega_1 a^2 \ , \tag{13}$$

which has been studied extensively in many cosmological DE models (Copeland et al. 2006). However, this representation in terms of the EoS parameter or energy density of the DE sector $\rho_\phi(z)$ are interrelated and one can consider any of these approaches to begin with.

At present, most of the existing models of DE lack a well motivated physical background which can explain the origin of late-time cosmic acceleration successfully, so it is reasonable to consider a phenomenological approach. Cosmologists are looking forward to the DESI (DESI Collaboration et al. 2016), *Euclid* (Laureijs et al. 2011) and LSST (Abell et al. 2009) experiments which, when operational, will provide high precision data. These efforts will be useful for understanding the expansion history of the universe and one will be able to verify the viability of various DE models beyond a ΛCDM model. Until then, one can test a cosmological toy model with the available data and check its viability. Motivated by these facts, in this paper, we made the ansatz (9) to track the expansion dynamics of the universe. The assumption in Equation (9) (or equivalently Eq. (10) or (11)) now makes the system of equations closed. In what follows, we shall try to obtain some cosmological solutions for this toy model providing an accelerating universe.

From Equations (1), (7) and (10), the expression for the Hubble parameter is obtained as

$$H^2 = H_0^2 \left\{ \Omega_{m0} a^{-3} + \frac{\beta \Omega_{\phi 0}}{(k+a)^\lambda} \exp\left[- \frac{k\lambda}{(k+a)} \right] \right\} , \tag{14}$$

where $\beta = (1+k)^\lambda \exp\left[\frac{k\lambda}{(1+k)}\right]$ is a constant. $\Omega_{m0} = \frac{\rho_{m0}}{3H_0^2}$ and $\Omega_{\phi 0} (= \frac{\rho_{\phi 0}}{3H_0^2}) = 1 - \Omega_{m0}$ represent the current values of density parameters for the matter and scalar fields respectively.

The deceleration parameter q is defined as

$$q = -\frac{\ddot{a}}{aH^2} = -\left(1 + \frac{\dot{H}}{H^2}\right) , \tag{15}$$

where $\dot{H} = \frac{dH}{dt} = aH\frac{dH}{da}$.

From Equations (14) and (15), we have obtained the expression for q in terms of scale factor a as,

$$q(a) = -1 + \frac{\frac{3}{2}\Omega_{m0} a^{-3} + \frac{\lambda \beta \Omega_{\phi 0} a^2}{2(k+a)^{\lambda+2}} \exp\left[-\frac{k\lambda}{(k+a)}\right]}{\Omega_{m0} a^{-3} + \frac{\beta \Omega_{\phi 0}}{(k+a)^\lambda} \exp\left[-\frac{k\lambda}{(k+a)}\right]} \ . \tag{16}$$

Now, Equation (16) can be written in terms of redshift z as

$$q(z) = -1 + \frac{\frac{3}{2}\Omega_{m0}(1+z)^3 + \frac{\lambda \beta \Omega_{\phi 0}(1+z)^\lambda}{2(1+k(1+z))^{\lambda+2}} \exp\left[-\frac{k\lambda(1+z)}{(1+k(1+z))}\right]}{\Omega_{m0}(1+z)^3 + \frac{\beta \Omega_{\phi 0}(1+z)^\lambda}{(1+k(1+z))^\lambda} \exp\left[-\frac{k\lambda(1+z)}{(1+k(1+z))}\right]} \ . \tag{17}$$

For the sake of completeness, we have also obtained the functional behavior of the density parameters for the matter field (Ω_m) and scalar field (Ω_ϕ) as:

$$\Omega_m(z) = \frac{\Omega_{m0}(1+z)^3}{\Omega_{m0}(1+z)^3 + \frac{\beta \Omega_{\phi 0}(1+z)^\lambda}{(1+k(1+z))^\lambda} \exp\left[-\frac{k\lambda(1+z)}{(1+k(1+z))}\right]} \ , \tag{18}$$

$$\Omega_\phi(z) = \frac{\beta \Omega_{\phi 0}(1+z)^\lambda \exp\left[-\frac{k\lambda(1+z)}{(1+k(1+z))}\right] (1+k(1+z))^{-\lambda}}{\Omega_{m0}(1+z)^3 + \frac{\beta \Omega_{\phi 0}(1+z)^\lambda}{(1+k(1+z))^\lambda} \exp\left[-\frac{k\lambda(1+z)}{(1+k(1+z))}\right]} \ . \tag{19}$$

Now, adding Equations (3) and (4), one can obtain

$$\begin{aligned}\dot{\phi}^2 =&(1+z)^2H^2\left(\frac{d\phi}{dz}\right)^2=(1+\omega_\phi(z))\rho_\phi(z)\\ \Rightarrow&\frac{d\phi(z)}{dz}=\pm\frac{\sqrt{\lambda}(1+z)^{-1}}{1+k(1+z)}\\ &\times\left\{1+\frac{\Omega_{m0}}{\beta\Omega_{\phi0}}\frac{(1+k(1+z))^\lambda}{(1+z)^{(\lambda-3)}}\right.\\ &\left.\times\exp\left[\frac{k\lambda(1+z)}{(1+k(1+z))}\right]\right\}^{-1/2},\end{aligned}\tag{20}$$

which on integration gives,

$$\begin{aligned}\phi(z)=&\phi_0\pm\left(\frac{2}{k}\right)^{\frac{\lambda}{2}}\lambda^{\frac{(1-\lambda)}{2}}\mathcal{F}(z)\\ &\times\frac{(1+z)^{-1}(1+k(1+z))^{\frac{\lambda}{2}}}{\sqrt{1+\frac{\Omega_{m0}}{\beta\Omega_{\phi0}}\frac{(1+k(1+z))^\lambda}{(1+z)^{-2}}\exp\left[-\frac{k\lambda(1+z)}{(1+k(1+z))}\right]}},\end{aligned}\tag{21}$$

where ϕ_0 is an integration constant and

$$\mathcal{F}(z)=\exp\left[\frac{k\lambda(1+z)}{2(1+k(1+z))}\right]\Gamma\left(\frac{\lambda}{2},\frac{k\lambda(1+z)}{2(1+k(1+z))}\right).$$

Similarly, using Equations (3) and (4), one can reconstruct the potential for the scalar field as

$$V(\phi)=\frac{1}{2}\rho_\phi(1-\omega_\phi)\ ,\tag{22}$$

which when expressed in terms of redshift parameter z becomes

$$\begin{aligned}V(z)=&V_0\frac{(1+z)^\lambda}{[1+k(1+z)]^\lambda}\\ &\times\left[1-\frac{\lambda}{6(1+k(1+z))^2}\right]\\ &\times\exp\left[-\frac{k\lambda(1+z)}{(1+k(1+z))}\right],\end{aligned}\tag{23}$$

where $V_0=3H_0^2\Omega_{\phi0}\beta$. Therefore, by using Equations (21) and (23), one can arrive at the expression for potential $V(\phi)$ if the values of k and λ are given. In this work, we first obtain constraints on k and λ using the observational datasets and from the best-fit values, we then reconstruct the functional form of $V(\phi)$ (see Sect. 4).

In order to facilitate the structure formation, an accelerating model of the universe should have a deceleration history in the past as well. So, the deceleration parameter q is an important factor in modeling the evolution history of our universe. For this reason, we shall try to analyze the behavior of q for this particular model.

3 DATA ANALYSIS

Here we shall fit the present model by using the SNIa dataset and observational data from the Hubble data survey. We present a brief summary of the data analysis method for each of the datasets.

For the SNIa dataset, we have used the recently released Union2.1 compilation data (Suzuki et al. 2012) of 580 data points. The corresponding χ^2 function is defined as (Nesseris & Perivolaropoulos 2005)

$$\chi^2_{\rm SN}=A-\frac{B^2}{C}\tag{24}$$

with

$$A=\sum_{i=1}^{580}\frac{[\mu^{\rm obs}(z_i)-\mu^{\rm th}(z_i)]^2}{\sigma_\mu^2(z_i)}\ ,\tag{25}$$

$$B=\sum_{i=1}^{580}\frac{[\mu^{\rm obs}(z_i)-\mu^{\rm th}(z_i)]}{\sigma_\mu^2(z_i)}\ ,\tag{26}$$

and

$$C=\sum_{i=1}^{580}\frac{1}{\sigma_\mu^2(z_i)}\ ,\tag{27}$$

where $\mu^{\rm obs}$ is the observed distance modulus at a particular redshift, $\mu^{\rm th}$ is the corresponding theoretical counterpart and σ_μ is the error.

Next, we have continued the analysis with 29 data points obtained in Hubble parameter measurements (Simon et al. 2005; Stern et al. 2010; Blake et al. 2012; Moresco et al. 2012; Chuang & Wang 2013; Samushia et al. 2013; Zhang et al. 2014; Delubac et al. 2015; Ding et al. 2015) in the range $0.07\le z\le 2.34$ (Mamon & Das 2015). The corresponding χ^2 function is given by

$$\chi^2_{\rm H}=\sum_{i=1}^{29}\frac{[h^{\rm obs}(z_i)-h^{\rm th}(z_i)]^2}{\sigma^2(z_i)}\ .\tag{28}$$

In the above equation, $h^{\rm obs}$ and $h^{\rm th}$ are the observed and theoretical values of the Hubble parameter respectively. Also, σ represents the error in Hubble parameter measurements and $h(z)=\frac{H(z)}{H_0}$.

Now the total χ^2 for the (SNIa+Hubble) dataset is defined as

$$\chi^2_{\rm total}=\chi^2_{\rm SN}+\chi^2_{\rm H}\ .\tag{29}$$

One can now minimize these χ^2 functions (i.e., $\chi^2_{\rm SN}$, $\chi^2_{\rm H}$ and $\chi^2_{\rm total}$) with respect to the model parameters and compute the estimated values and their errors.

4 RESULTS

Following the data analysis method mentioned above, in this section, limits on the values of k and λ are obtained for the Hubble, SNIa and Hubble+SNIa datasets, which are displayed in Table 1 along with the 1σ errors.

Table 1 Best fit values for k and λ for the Hubble and SNIa Datasets with $\Omega_{m0} = 0.27$. Here, χ^2_m represents the minimum value of χ^2.

Dataset	k	λ	χ^2_m (min. value of χ^2)
Hubble	4.96 ± 0.40	2.82 ± 0.23	28.59
SNIa	4.97 ± 0.22	2.99 ± 0.19	562.27
SNIa+Hubble	4.93 ± 0.10	2.94 ± 0.12	573.84

It has been found that the joint analysis of the SNIa+Hubble dataset puts a tighter constraint as compared to the constraints obtained from the SNIa or Hubble datasets alone. Using these values, the deceleration parameter $q(z)$ has been reconstructed for different datasets which are shown in Figure 1.

From Figure 1, we have found that $q(z)$ enters into a negative value regime in the recent past at a redshift z_t. The best-fit values of $q(z)$ at present (say, $q_0 = q(z = 0)$) and the redshift z_t at which a transition in q occurs along with 1σ errors for different datasets are listed in Table 2.

Table 2 Best fit values of q_0 and z_t (within 1σ errors) for different datasets.

Datasets	q_0	z_t
Hubble	$q_0 = -0.57 \pm 0.13$	$z_t = 0.75 \pm 0.04$
SNIa	$q_0 = -0.56 \pm 0.05$	$z_t = 0.76 \pm 0.02$
SNIa+Hubble	$q_0 = -0.56 \pm 0.02$	$z_t = 0.76 \pm 0.01$

These results are almost consistent with known values for the flat ΛCDM model ($q_0 = -0.59$, $z_t = 0.75$) with $\Omega_{m0} = 0.27$ and $\Omega_{\Lambda 0} = 0.73$. It deserves mention that our results also match those obtained in literature [for details, one can examine Turner & Riess (2002); Riess et al. (2004); Cunha (2009); Mamon & Das (2016) and references therein].

Figure 2 shows the future evolution of $q(z)$. It is evident from Figure 2 that the present model does not indicate any slowing down of the present cosmic acceleration in the near future as suggested in Shafieloo et al. (2009); Magaña et al. (2014) for various DE parametrizations. In the far future (near $z \to -1$), however there is evidence that the rate of expansion varies but the universe continues to accelerate forever in the present toy model. Hence, we need more robust observational datasets and more effective analysis methods to have consensus on whether the cosmic acceleration is speeding up or not.

The reconstructed evolution dynamics of $\omega_\phi(z)$ is shown in Figure 3 for different datasets. The values of $\omega_\phi(z)$ at present (i.e., $\omega_\phi(z = 0)$) with 1σ errors for the Hubble, SNIa and SNIa+ Hubble datasets are obtained as -0.88 ± 0.26, -0.89 ± 0.10 and -0.89 ± 0.04 respectively.

In the left panel of Figure 4, we depict the behavior of $\omega_\phi(z)$ for the values of k and λ obtained in Table 1 for each dataset. We also plot the rate of change of ω_ϕ against z $\left(D = \frac{d\omega_\phi}{dz}\right)$ in Figure 4, which shows that the magnitude of $\frac{d\omega_\phi}{dz}$ is negative and remains almost constant at high redshifts, but the magnitude of $\frac{d\omega_\phi}{dz}$ is decreasing at low redshifts for each dataset.

Figures 3 and 4 indicate that at high redshifts the present model does not have any significant deviation from the ΛCDM model, but with evolution (as $z \to 0$), the deviation from ΛCDM becomes prominent. This dynamical nature of the DE component can be effective in determining the late time evolution of the universe and thus may provide an answer to the *coincidence problem* in cosmology.

For the sake of completeness, we have also solved Equations (21) and (23) numerically and plotted the potential $V(\phi)$ for $k = 4.93$, $\lambda = 2.94$, $\Omega_{\phi 0} = 0.73$, $H_0 = 72\ \mathrm{km\ s^{-1}\,Mpc^{-1}}$ and $\phi_0 = 5$ in the left panel of Figure 5. From this figure, we have found that the potential $V(\phi)$ increases with ϕ. The reason behind this seems to be the choice of ρ_ϕ as given in Equation (9). For this toy model, $V(\phi)$ can be obtained as

$$V(\phi) \approx A\exp(\alpha_1\phi) + B\exp(\alpha_2\phi)\ , \qquad (30)$$

where $A = 1.07 \times 10^4$, $\alpha_1 = 0.02$, $B = -4.21 \times 10^{16}$ and $\alpha_2 = -9.50$. Recently, this type of potential has already been discussed by several authors while explaining the late-time cosmic acceleration (Barreiro et al. 2000; Rubano & Scudellaro 2001; Sen & Sethi 2002). We have also checked that the nature of the $V(\phi)$ curve is hardly affected by a small change in the allowed values of k and λ within the 1σ confidence limit and other choices of ϕ_0.

The variation of density parameters $\Omega_m(z)$ and $\Omega_\phi(z)$ is also shown in the right panel of Figure 5. This plot also indicates that the universe has evolved to a DE dominated era in the recent past, which is in accordance with observational results.

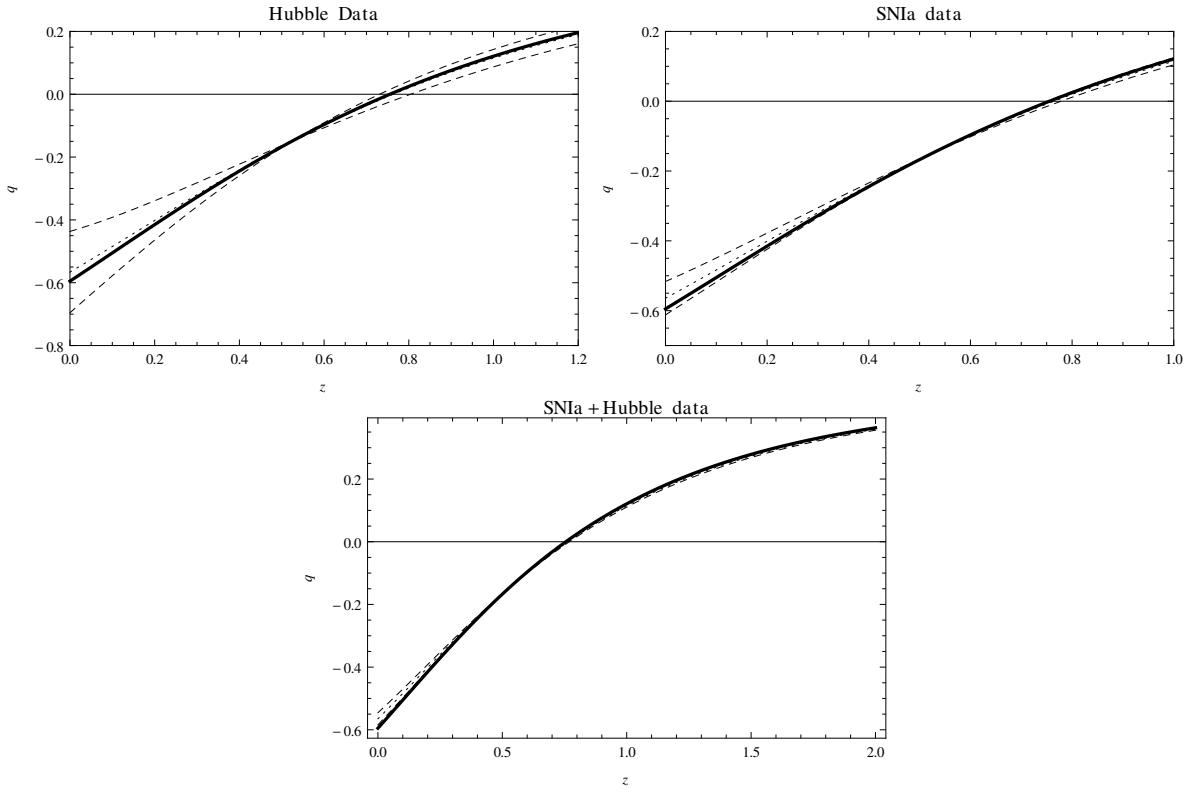

Fig. 1 The reconstructed $q(z)$ values for different observational datasets are shown. For each panel, the *central dotted line* and the *dashed lines* represent the best-fit curve with 1σ errors respectively. Also, in each panel, the *thick line* indicates a ΛCDM universe (with $\Omega_{m0} = 0.27$ and $\Omega_{\Lambda 0} = 0.73$). This is for $\Omega_{m0} = 0.27$.

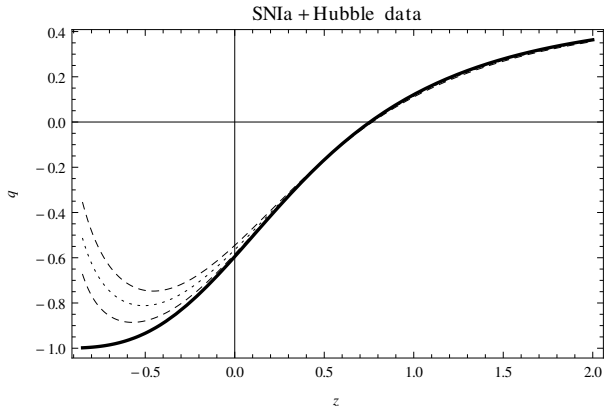

Fig. 2 Future evolution of $q(z)$ for this model shown by a *dotted line* along the 1σ contour (*dashed lines*). This plot corresponds to values of (k, λ) obtained for the SNIa+Hubble dataset with $\Omega_{m0} = 0.27$. The *thick line* as usual indicates the behavior of q for ΛCDM model.

5 GROWTH OF PERTURBATIONS

We are also interested in looking into the effect of this particular DE sector on the evolution of matter overdensities. It is expected that the growth of matter perturbations will be affected in the presence of a DE sector. As the DE sector provides a repulsive gravity effect, it will result in slowing down growth of the matter sector. However, for different DE models the effect will be different depending upon the nature of the DE EoS parameter. In this section we want to study the rate by which the evolution of matter densities gets affected for this particular form of DE density. To study this, we consider the following sys-

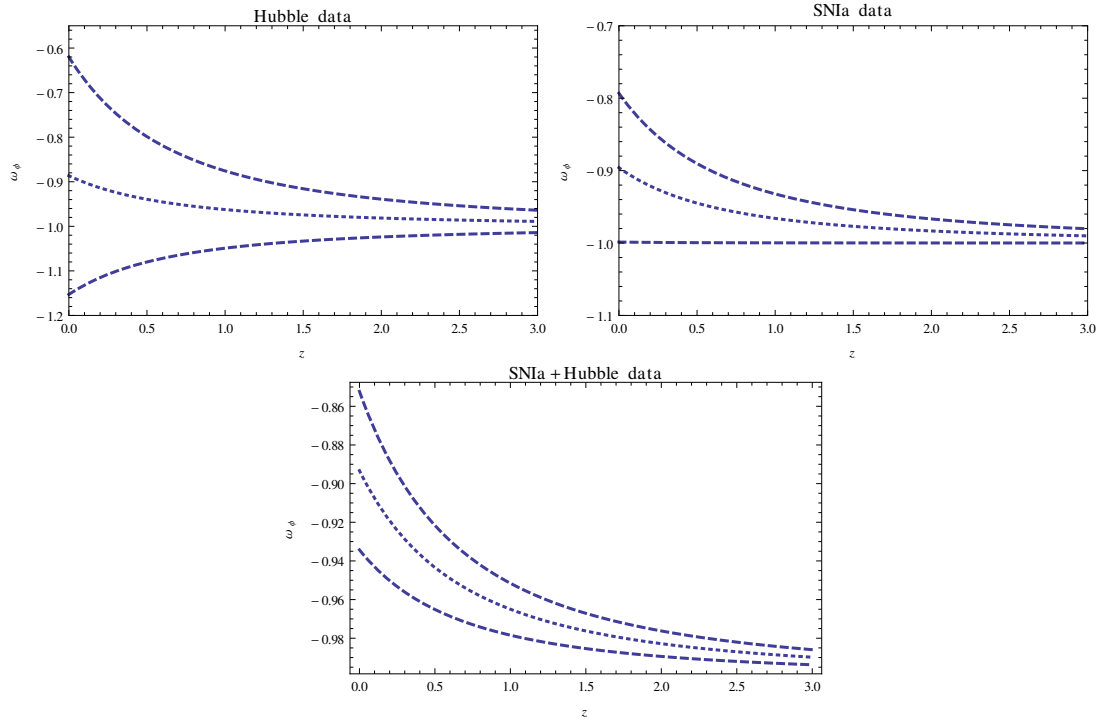

Fig. 3 The reconstructed EoS parameter $\omega_\phi(z)$ for this model using various observational datasets, as indicated in each panel. The *central dotted line* represents the best-fit curve and the *dashed lines* signify the 1σ contour. All the plots are for $\Omega_{m0} = 0.27$.

tem of linearized Einstein Equations (Jaber & Macorra 2018)

$$a^2\delta_m''(a)+a\frac{3}{2}\left[1-\omega_\phi(a)\Omega_\phi(a)\right]\delta_m'(a) -\frac{3}{2}\left[\Omega_m(a)\delta_m(a)+\Omega_\phi(a)\delta_\phi(a)\right]=0\ , \tag{31}$$

$$a^2\delta_\phi''(a)+a\frac{3}{2}\left[1-\omega_\phi(a)\Omega_\phi(a)\right]\delta_\phi'(a) +\left[\frac{c_s^2\kappa^2}{a^2H^2(a)}-\frac{3}{2}\Omega_\phi(a)\right]\delta_\phi(a) -\frac{3}{2}\Omega_m(a)\delta_m(a)=0\ , \tag{32}$$

where

$$\delta_m \equiv \frac{\delta\rho_m}{\rho_m} \quad \text{and} \quad \delta_\phi \equiv \frac{\delta\rho_\phi}{\rho_\phi}$$

represent the matter and DE density contrasts, respectively. A prime indicates variation with respect to a and κ is the Fourier wave number. Also, the term c_s^2 in Equation (32) represents the speed of sound for the DE sector. One can split it into the sum of an adiabatic and an effective (non-adiabatic) contribution, namely $c_{\rm ad}^2$ and $c_{\rm eff}^2$ respectively, given by

$$c_s^2 = \frac{\delta p_\phi}{\delta\rho_\phi} = c_{\rm ad}^2 + c_{\rm eff}^2\ , \tag{33}$$

where

$$c_{\rm ad}^2 = \omega_\phi - \frac{1}{3}\frac{\dot{\omega}_\phi}{H(1+\omega_\phi)} = \omega_\phi(a) - \frac{1}{3}\frac{a\omega_\phi'(a)}{(1+\omega_\phi(a))}.$$

Following Jaber & Macorra (2018), in this work, we have modeled $c_{\rm eff}^2$ as a constant which can take values $c_{\rm eff}^2 = 0,\ \frac{1}{3}$ or 1.

To solve this system of equations, we need initial conditions for δ_m and δ_ϕ. For our case, we set our initial conditions at the matter dominant era when the DE contribution was very small and the modes are well inside the horizon. We choose $\delta_m(a_{\rm ini}) = 10^{-5}$ at $\kappa = 0.01\,{\rm Mpc}^{-1}$, which corresponds to the value when the κ-mode enters the horizon. For the scalar field perturbation, the contribution from the DE sector is considered to be negligible initially and is set at $\delta_\phi(a_{\rm ini}) = 10^{-8}$.

With the initial conditions mentioned above, the system of equations is solved numerically for different values of $c_{\rm eff}^2$. We have displayed the results in Figure 6 for $c_{\rm eff}^2 = 1$. However, it has been found that the different values of $c_{\rm eff}^2$ only reduce the growth of matter overdensities slightly, keeping the shape the same. In Figure 6, the solid line represents the growth of matter perturbations for the present DE model, which is slower compared to the growth rate when there is no DE compo-

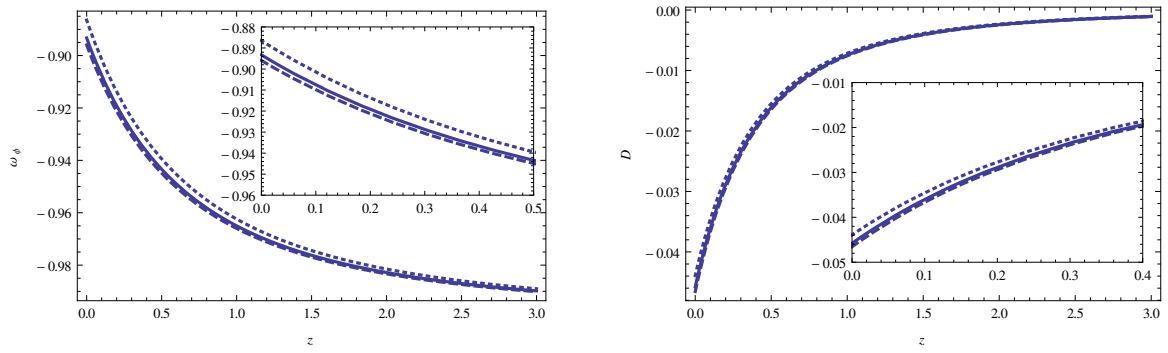

Fig. 4 The left panel shows a plot of the reconstructed EoS parameter $\omega_\phi(z)$ using the best-fit values of k, λ and $\Omega_{m0} = 0.27$. The right panel displays a plot of $D\left(= \frac{d\omega_\phi}{dz}\right)$ against z. In both plots, the *dotted*, *dashed* and *thick lines* represent the evolution of the corresponding parameter for the Hubble, SNIa and SNIa+Hubble datasets respectively.

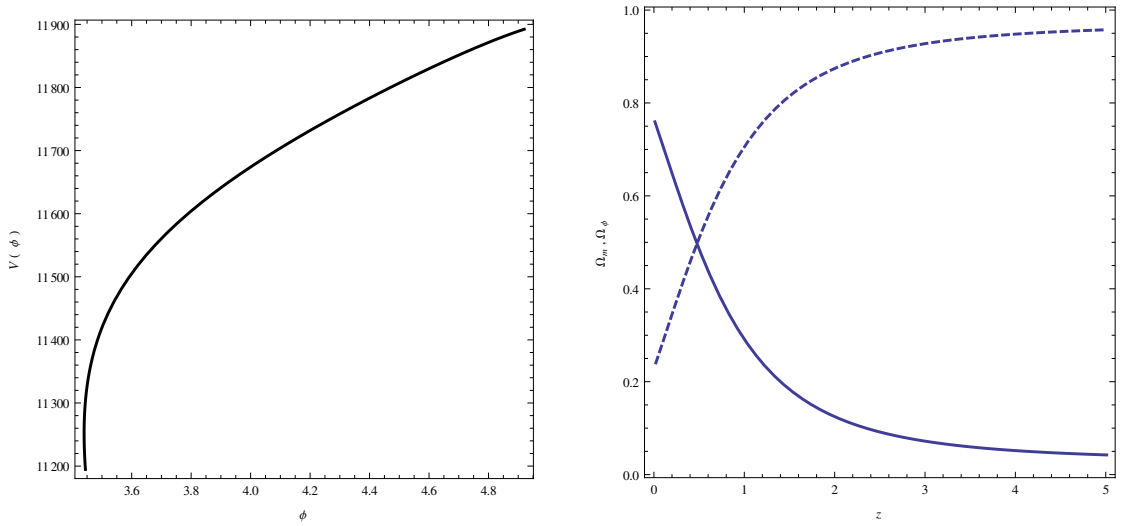

Fig. 5 The left panel shows the reconstructed potential $V(\phi)$ with (k, λ) values arising from the SNIa+Hubble dataset. In this plot, we have chosen $\Omega_{\phi 0} = 0.73$, $H_0 = 72\,\mathrm{km\ s^{-1}\ Mpc^{-1}}$ and $\phi_0 = 5$. The right panel displays the plot of Ω_m (*dashed curve*) and Ω_ϕ (*solid curve*) for $k = 4.9$, $\lambda = 2.9$ and $\Omega_{m0} = 0.27$.

nent in the universe (shown by the dotted line in Fig. 6). We have also compared the growth rate for our model with that for a ΛCDM model ($\omega_{\Lambda\mathrm{CDM}} = -1$) and CPL model ($\omega_{\mathrm{CPL}} = \omega_0 + \frac{\omega_1 z}{(1+z)}$) (Chevallier & Polarski 2001; Linder 2003) (shown by orange and green lines respectively). For the CPL model, the values of ω_0 and ω_1 have been taken as $\omega_0 = -1.17$ and $\omega_1 = 0.35$ (Qi et al. 2016) respectively. It is evident that with evolution (increasing a), the effect of the present DE sector on the growth of matter overdensities is larger as compared to a ΛCDM or a CPL model.

In Figure 7 we have plotted the percentage deviation in the growth rate for the present model compared to a no DE model. We have actually plotted the percentage decrease in the growth rate given by $\Delta_m = \frac{\delta_m - \delta_{m(\mathrm{noDE})}}{\delta_{m(\mathrm{noDE})}}$. The higher the percentage decrease is, the slower the growth rate is. It is evident from the figure that the growth rate becomes slower with the evolution and at later times when the DE component dominates the evolution, the growth rate is suppressed by around 12%.

6 CONCLUSIONS

To summarize, in this paper, we have tried to show that a canonical scalar field model can provide an early decelerated expansion followed by an accelerated expansion at late times. For this purpose, we have chosen one specific ansatz for ρ_ϕ to characterize the properties of

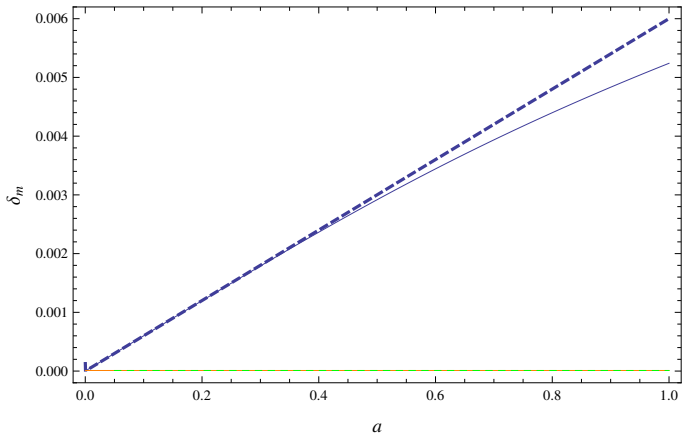

Fig. 6 Growth of matter overdensities $\delta_m(a)$ for $c_s^2 = 1$. The *solid line* represents the growth of perturbations for the present DE model whereas the *dashed line* signifies the growth rate in absence of DE. The *orange* and *green lines* trace $\delta_m(a)$ for the ΛCDM and CPL models respectively (*color online*). In this plot, we have chosen $H_0 = 72\,\mathrm{km\,s^{-1}\,Mpc^{-1}}$ and the values of the model parameters k and λ have been taken from joint analysis of the SNIa + Hubble dataset as listed in Table 1.

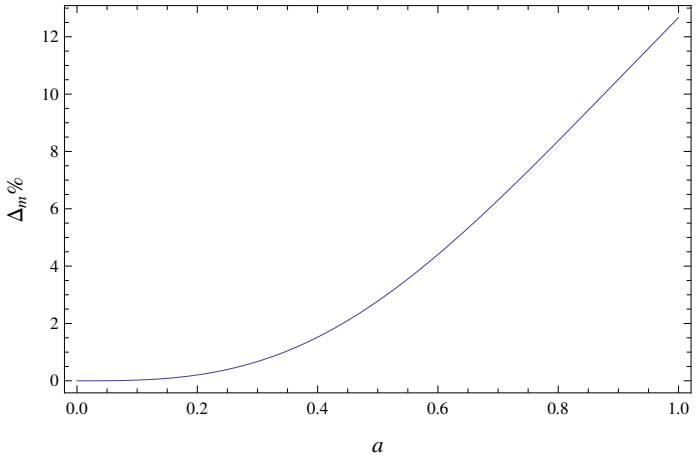

Fig. 7 Percentage decrease in δ_m as a function of scale factor compared to a no DE model.

DE. Then with this input, we have obtained exact analytical solutions for various cosmological parameters. Using the SNIa, Hubble and SNIa+Hubble datasets, we have reconstructed the deceleration parameter $q(z)$ and the EoS parameter $\omega_\phi(z)$ of this model. Results indicate that the evolution of $q(z)$ does not provide any signal of cosmic deceleration in the future. The reconstructed values of q_0, z_t and $\omega_\phi(z = 0)$ have been calculated and it has been found that the results obtained do not deviate much from the standard ΛCDM model. Furthermore, the potential $V(\phi)$ has been found numerically for some specific choices of model parameters and the potential is found to be a combination of two exponentials in ϕ (see Eq. (30)). As already discussed, this type of potential has earlier been considered by several authors for quintessence fields. Hence, this work shows again the importance of the double exponential potential for a quintessence field. Finally, we would like to mention that the observational datasets suffer from systematic errors and the reconstructed results might vary for other datasets. So, one can hope that the next generation of observational datasets will improve the constraints on these model parameters considerably.

From the perturbative analysis it has been found that the dynamical evolution of the DE sector or the corresponding EoS parameter $\omega_\phi(z)$ got imprinted in the growth rate of the matter sector and this effect is much more prominent at later times for the present DE model as compared to a ΛCDM model or a CPL model.

However, as nothing much is known about the DE sector and a wide variety of possibilities is open, various effective cosmological toy models can be considered for different functional forms for ρ_ϕ, which may agree even better with the observational results. So, one effective way to check the viability of a DE model may be to look at the imprints of these models on the growth rate of matter perturbations and compare it with available experimental measurements.

Acknowledgements SD and MB acknowledge financial support from SERB, DST, Government of India, through the project EMR/2016/007162. SD would also like to acknowledge IUCAA, Pune for providing support through the associateship programme. AAM acknowledges financial support from SERB, Government of India through the National Post-Doctoral Fellowship Scheme (File No: PDF/2017/000308) and the Department of Physics, Visva-Bharati where a part of the work was completed.

References

Abell, P. A., Burke, D. L., Hamuy, M., et al. 2009, Lsst Science Book, version 2.0, Tech. rep., LSST Science Collaboration

Barreiro, T., Copeland, E. J., & Nunes, N. J. 2000, Phys. Rev. D, 61, 127301

Bartolo, N., Corasaniti, P.-S., Liddle, A. R., & Malquarti, M. 2004, Phys. Rev. D, 70, 043532

Blake, C., Brough, S., Colless, M., et al. 2012, MNRAS, 425, 405

Chevallier, M., & Polarski, D. 2001, International Journal of Modern Physics D, 10, 213

Choudhury, T. R., & Padmanabhan, T. 2005, A&A, 429, 807

Chuang, C.-H., & Wang, Y. 2013, MNRAS, 435, 255

Copeland, E. J., Sami, M., & Tsujikawa, S. 2006, International Journal of Modern Physics D, 15, 1753

Cunha, J. V. 2009, Phys. Rev. D, 79, 047301

Delubac, T., Bautista, J. E., Busca, N. G., et al. 2015, A&A, 574, A59

DESI Collaboration, Aghamousa, A., Aguilar, J., et al. 2016, The DESI Experiment Part I : Science, Targeting and Survey Design (arXiv:1611.00036)

Ding, X., Biesiada, M., Cao, S., Li, Z., & Zhu, Z.-H. 2015, ApJ, 803, L22

Eisenstein, D. J., Zehavi, I., Hogg, D. W., et al. 2005, ApJ, 633, 560

Jaber, M., & Macorra, A. d. l. 2018, Astroparticle Physics, 97, 130

Jassal, H. K. 2010, Phys. Rev. D, 81, 083513

Laureijs, R., Amiaux, J., Arduini, S., et al. 2011, Euclid Definition Study Report, arXiv:1110.3193

Linder, E. V. 2003, Physical Review Letters, 90, 091301

Magaña, J., Cárdenas, V. H., & Motta, V. 2014, J. Cosmol. Astropart. Phys., 10, 017

Mamon, A. A., & Das, S. 2015, European Physical Journal C, 75, 244

Mamon, A. A., & Das, S. 2016, International Journal of Modern Physics D, 25, 1650032

Martin, J. 2008, Modern Physics Letters A, 23, 1252

Moresco, M., Cimatti, A., Jimenez, R., et al. 2012, J. Cosmol. Astropart. Phys., 8, 006

Nesseris, S., & Perivolaropoulos, L. 2005, Phys. Rev. D, 72, 123519

Padmanabhan, T., & Choudhury, T. R. 2003, MNRAS, 344, 823

Perlmutter, S., Aldering, G., Goldhaber, G., et al. 1999, ApJ, 517, 565

Qi, J.-Z., Zhang, M.-J., & Liu, W.-B. 2016, arXiv:1606.00168

Riess, A. G., Filippenko, A. V., Challis, P., et al. 1998, AJ, 116, 1009

Riess, A. G., Nugent, P. E., Gilliland, R. L., et al. 2001, ApJ, 560, 49

Riess, A. G., Strolger, L.-G., Tonry, J., et al. 2004, ApJ, 607, 665

Rubano, C., & Scudellaro, P. 2001, astro-ph/0103335

Sahni, V. 2004, in Lecture Notes in Physics, 653, ed. E. Papantonopoulos, (Berlin: Springer Verlag) 141

Sahni, V., & Starobinsky, A. 2000, International Journal of Modern Physics D, 9, 373

Samushia, L., Reid, B. A., White, M., et al. 2013, MNRAS, 429, 1514

Sen, A. A., & Sethi, S. 2002, Physics Letters B, 532, 159

Shafieloo, A., Sahni, V., & Starobinsky, A. A. 2009, Phys. Rev. D, 80, 101301

Simon, J., Verde, L., & Jimenez, R. 2005, Phys. Rev. D, 71, 123001

Spergel, D. N., Bean, R., Doré, O., et al. 2007, ApJS, 170, 377

Steinhardt, P. J., Wang, L., & Zlatev, I. 1999, Phys. Rev. D, 59, 123504

Stern, D., Jimenez, R., Verde, L., Kamionkowski, M., & Stanford, S. A. 2010, J. Cosmol. Astropart. Phys., 2, 008

Suzuki, N., Rubin, D., Lidman, C., et al. 2012, ApJ, 746, 85

Turner, M. S., & Riess, A. G. 2002, ApJ, 569, 18

Unnikrishnan, S. 2008, Phys. Rev. D, 78, 063007

Unnikrishnan, S., Jassal, H. K., & Seshadri, T. R. 2008, Phys. Rev. D, 78, 123504

Weinberg, S. 1989, Reviews of Modern Physics, 61, 1

Weller, J., & Lewis, A. M. 2003, MNRAS, 346, 987

Zhang, C., Zhang, H., Yuan, S., et al. 2014, RAA (Research in Astronomy and Astrophysics), 14, 1221